ISSN (e): 2250 – 3005 || Volume, 07 || Issue, 11|| November – 2017 ||
International Journal of Computational Engineering Research (IJCER)

Effect of radiation on MHD nanofluid flow considering effective thermal conductivity and viscosity due to Brownian motion

Dr. Hari R. Kataria[1,] Mrs. Mital H. Mistry[2,*]

[1] *Department Of Mathematics, Faculty of Science, The M. S. University of Baroda, Vadodara-390002, India,*
[2] *Department Of Mathematics, Faculty of Science, The M. S. University of Baroda, Vadodara-390002, India*
Corresponding Author: Dr. Hari R. Kataria

ABSTRACT

This study is concerned with the effect of radiation on flow, heat and mass transfer of Nanofluid flow past over an oscillating vertical plate. Effect of Brownian motion on thermal conductivity and viscosity of nanofluid is considered. Thus effects of nano particle size, volume fraction, temperature, types of nano particle and base fluid combinations are taken into consideration. Specifically we have considered CuO-Water nanofluid. Effect of thermal interfacial thermal resistance is also considered. The governing system of partial differential equations are converted into non-dimensional system and then solved analytically. Flow characteristics are analyzed graphically and the physical aspects are discussed in detail. Skin friction, Nusselt number and Sherwood number are also derived and represented through tables.

Keywords: MHD, Radiation, Nanofluid, Analytic solution, Isothermal, Ramped, Brownian motion.

Date of Submission: 31-10-2017 Date of acceptance: 09-11-2017

Nomenclature

T	Temperature
T_w	Constant temperature
u	Velocity
C	Concentration
D	Mass diffusivity
B	External uniform magnetic field
B_0	Constant magnetic flux density
Cp	Specific heat at constant pressure
t	Time
g	Acceleration due to gravity
k	Thermal conductivity
M	Magnetic parameter
Pr	Prandtl number
Sc	Schmidt number
Gr	Grashof number
Gm	Grashof number of mass transfer

Greek letters

σ	electric conductivity of the fluid
ϕ	porosity of the fluid
Ø	Nanoparticle volume fraction
β	volumetric coefficient of thermal expansion
ρ	Density
k	Thermal conductivity
ν	Kinematic viscosity

Subscripts

f	Fluid phase
nf	Nano-fluid
s	Solid phase

I. INTRODUCTION

Magnetohydrodynamic (MHD) has many applications in sciences and engineering. The interaction between magnetic field and electrically conducting fluid have significant effect on various equipment such as bearings, pumps and generators. Thus scientists are attracted towards study of MHD fluid flow. Narahari et al. [1] modelled unsteady viscous flow with ramped wall temperature. Transient free convection in the presence of thermal radiation was studied by Narahari [2]. Narahari and Sulaiman [3] discussed thermal radiation effects on unsteady MHD natural convection. Nadeem et al. [4] investigated MHD flow over an exponentially shrinking sheet. Seth et al. [5-12] analyzed effects of Thermal Radiation, Rotation and Hall Current on MHD in the Presence of Thermal Diffusion with Heat Absorption while Seth and Sarkar [13] took care of time Dependent Moving Vertical Plate. Narahari et al. [14] studied Dufour effects on MHD. Seth et al. [15] explained fluid flow with variable ramped temperature. Many interesting MHD flow problems can be found in [16-19]. Kataria and Patel [20-23] studied MHD flow taking different types of Non-Newtonian fluids. Kataria et al. [24] discussed flow of a micropolar fluid between two vertical walls. Hayat et al. [25] considered burgers fluid flow problem.

Liquids have lower thermal conductivity than solids. Heat transfer can be enhanced by suspension of nano sized solid particles (like copper) in the conventional base fluid (water or engine oil). Such type of fluids are known as nanofluids. Sheikholeslami and Ganji [26] discussed Cu-water nanofluid flow and Sheikholeslami et al. [27-29] simulated MHD nanofluid flow considering effects of various pertinent parameters. Kataria and Mittal [30] derived Mathematical model for optically thick nanofluid flow. Sheri and Thumma [31-32] investigated heat and Mass Transfer Effects on nanofluid flow. Effect of micromixing on nanofluid flow was carried out by Sheikholeslami et al. [33]. Kataria and Mittal [34] studied velocity, mass and temperature profiles of nanofluid flow. Recent work [35-44] are considering different types of nanofluids and applications such as modelling of blood flow which may help us to understand effects of radiation and magnetic field on blood.

The aim of this article is to investigate the gravity-driven convective boundary layer flow of nanofluids. In most of the previous work, effect the Brownian motion on thermal conductivity and viscosity is neglected. So we have considered it our present work. Also bounding plate with ramped temperature and ramped surface concentration as well as case of isothermal temperature and ramped surface concentration are considered. The governing dimensionless equations are solved analytically and presented in closed form.

II. MATHEMATICAL FORMULATION OF THE PROBLEM

A Cartesian coordinate system (x, y) is considered such that x-axes is along the plate and the y-axes is perpendicular to it. The flow is restricted to y > 0. The fluid is electrically conducting with a uniform magnetic field B0 along y axes. Induced magnetic field produced is neglected. The fluid is a single phase nanofluid like water based fluid containing copper (or silver) as nanoparticles. Physical sketch of the problem is shown in Fig. 1

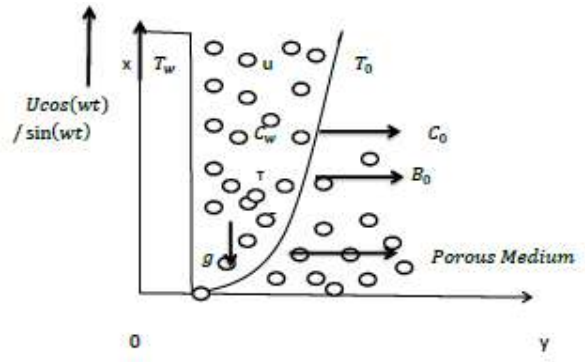

Figure 1. Physical sketch of the problem

For the problem under consideration, we assume the velocity $V = u(y,t)$ along $x - axis$. Under above assumptions and governing equations (Boussinesq approximation) are given below:

$$\rho_{nf}\frac{\partial u}{\partial t} = \mu_{nf}\frac{\partial^2 u}{\partial y^2} - \sigma_{nf}B^2 u - \frac{\mu_{nf}\varphi}{k_1}u + g(\rho\beta)_{nf}(T - T_0) + g(\rho\beta_C)_{nf}(C - C_0) \quad (1)$$

$$(\rho c_p)_{nf}\frac{\partial T}{\partial t} = k_{nf}\frac{\partial^2 T}{\partial y^2} - \frac{\partial q_r}{\partial y} \quad (2)$$

$$\frac{\partial C}{\partial t} = D\frac{\partial^2 C}{\partial y^2} \quad (3)$$

Where [45]

$$\rho_{nf} = (1 - \emptyset)\rho_f + \emptyset\rho_s$$

$$\sigma_{nf} = \sigma_f\left[1 + \frac{3(\sigma-1)\emptyset}{(\sigma+2)-(\sigma-1)\emptyset}\right], \sigma = \frac{\sigma_s}{\sigma_f}$$

$$(\rho\beta)_{nf} = (1-\emptyset)(\rho\beta)_f + \emptyset(\rho\beta)_s$$

The Brownian motion plays vital role on thermal conductivity. Thus thermal conductivity proposed by Koo and Kleinstreuer [46-47] takes effects of solute (nano particle) size, solute volume fraction, temperature, types of nano particle and base fluid combinations into consideration. It is given as:

$$k_{nf} = k_{static} + k_{Brownian},$$

$$k_{static} = k_f\left[1 - 3\frac{\emptyset(k_f - k_{s,R})}{2k_f + k_{s,R} + \emptyset(k_f - k_{s,R})}\right]$$

$$\frac{1}{k_{s,R}} = \frac{1}{k_s} + \frac{R_f}{d_s}$$

$R_f = 4 * 10^{-9} Km^2/W$ is thermal interfacial resistance.

$$k_{Brownian} = 5 * 10^4 \emptyset \rho c_{p_f}\sqrt{\frac{k_b T}{(\rho d)_s}}\, g'(T, \emptyset, d_s)$$

$$g'(T, \emptyset, d_s) = \left(a_1 + a_2\ln(d_s) + a_3\ln(\emptyset) + a_4\ln(\emptyset)\ln(d_s) + a_5\ln(d_s^2)\right)\ln(T) + \left(a_6 + a_7\ln(d_s) + a_8\ln(\emptyset) + a_9\ln(\emptyset)\ln(d_s) + a_{10}\ln(d_s^2)\right)$$

$a_1 = -26.593310846,\ a_2 = -0.403818333,$
$a_3 = -33.3516805,\ a_4 = -1.915825591,$
$a_5 = 0.0642185846658,\ a_6 = 48.40336955$
$a_7 = -9.787756683,\ a_8 = 190.245610009,$
$a_9 = 10.9285386565,\ a_{10} = -0.72009983664$

(Here it must be noted that these values are not general and vary with nanofuid, the nanofluid in this article is Cu-water nanofluid.)

$$(\rho c_p)_{nf} = (1-\emptyset)(\rho c_p)_f + \emptyset(\rho c_p)_s$$

Considering effect of "micro mixing in suspensions" on viscosity [46], we get

$$\mu_{nf} = \mu_{static} + \mu_{Brownian} = \frac{\mu_f}{(1-\emptyset)^{2.5}} + \frac{k_{Brownian}*\mu_f}{k_f * Pr_f}$$

$$q_r = -\frac{4\sigma^*}{3k^*}\frac{\partial T^4}{\partial y}$$

Considering temperature difference within the flow to be sufficiently small, Using Taylor series and neglecting higher terms, q_r [48] becomes

$$q_r = -\frac{4\sigma^*}{3k^*}\frac{\partial(4T_0^{\,3}T - 3T_0^{\,4})}{\partial y}$$

Using this q_r in (2)

$$(\rho c_p)_{nf}\frac{\partial T}{\partial t} = (k_{nf} + \frac{16\sigma^* T_0^{\,3}}{3k^*})\frac{\partial^2 T}{\partial y^2} \qquad (4)$$

The initial and boundary conditions are

$$u = 0, \quad T = T_0, \quad C = C_0;\ as\ y \geq 0\ and\ t < 0$$

$$u = u_0 sin\omega t\ or\ u = u_0 cos\omega t$$

$$T = \begin{cases} T_0 + (T_w - T_0)\,{}^{t}/_{t_0} & if\ \ 0 < t < t_0 \\ T_w & if\ \ t \geq t_0 \end{cases},$$

$$C = \begin{cases} C_0 + (C_w - C_0)\,{}^{t}/_{t_0} & if\ \ 0 < t < t_0 \\ C_w & if\ \ t \geq t_0 \end{cases},\ as\ \ t \geq 0\ and\ y = 0$$

$$u \to 0, T \to T_0, \quad C \to C_0;\ as\ \ y \to \infty\ and\ t \geq 0$$

Introducing non-dimensional variables

$$y^* = \frac{u_0 y}{v_f}, t^* = \frac{u_0^{\,2} t}{v_f}, u^* = \frac{u}{u_0}, \theta = \frac{T - T_0}{T_w - T_0}, \omega^* = \frac{v_f \omega}{u_0^{\,2}}$$

(1) and (11) become (omitting * for simplicity)

$$\frac{\partial u}{\partial t} = a_1\frac{\partial^2 u}{\partial y^2} - \left(a_3 M^2 + \frac{a_1}{k}\right)u + G_r a_2\theta + G_m a_5 C \qquad (5)$$

$$\frac{\partial \theta}{\partial t} = a_4\frac{\partial^2 \theta}{\partial y^2} \qquad (6)$$

$$\frac{\partial c}{\partial t} = \frac{1}{s_c}\frac{\partial^2 c}{\partial y^2} \tag{7}$$

With initial and boundary condition

$$u = \theta = C = 0\,, \qquad y \geq 0, t = 0$$

$$u = \sin(wt)\, or \cos(wt)\,,$$

$$\theta = \begin{cases} t, & 0 < t \leq 1 \\ 1 & t > 1 \end{cases} = tH(t) - (t-1)H(t-1),$$

$$C = \begin{cases} t, & 0 < t \leq 1 \\ 1 & t > 1 \end{cases} = tH(t) - (t-1)H(t-1),$$

as $y = 0,\ t > 0$

$$u \to 0, \theta \to 0, C \to 0 \quad as\ y \to \infty, t > 0 \tag{8}$$

where

$$Pr = \frac{\mu\, c_p}{k}, M^2 = \frac{\sigma {B_0}^2}{\rho {u_0}^2} t_0, \qquad \frac{1}{k} = \frac{v\varphi^2}{k_1 {u_0}^2}, Gr = \frac{vg\beta(T_w - T_\infty)}{{u_0}^3},$$

$$Sc = \frac{v}{D}, Gm = \frac{g\beta_c v(C_w - C_\infty)}{{u_0}^3}$$

$$b_0 = 1 - \emptyset$$

$$b_1 = (b_0 + \emptyset \frac{\rho_s}{\rho_f}),$$

$$b_2 = (b_0 + \emptyset \frac{(\rho\beta)_s}{(\rho\beta)_f}),$$

$$b_3 = (b_0 + \emptyset \frac{(\rho c_p)_s}{(\rho c_p)_f}),$$

$$b_4 = \frac{k_{nf}}{k_f},$$

$$b_5 = \frac{\sigma_{nf}}{\sigma_f},$$

$$b_6 = \frac{b_4}{b_2},$$

$$b_7 = (b_0 + \emptyset \frac{(\rho\beta)_c}{(\rho\beta)_f}),$$

$$a_1 = \frac{1}{{b_0}^{2.5} b_1},$$

$$a_2 = \frac{b_2}{b_1},$$

$$a_3 = \frac{b_5}{b_1},$$

$$a_4 = \frac{b_4 + Nr}{b_2 pr},$$

$$a_5 = \frac{b_7}{b_1}$$

H (.) is Heaviside unit step function.

III. SOLUTION OF THE PROBLEM

Taking Laplace transform of equation (5) and (7) with initial and boundary condition equation(8)

$$\bar{\theta} = (1 - e^{-s}) F_8(y, s) \tag{9}$$

$$\bar{C} = F_{11}(y, s)(1 - e^{-s}) \tag{10}$$

$$\bar{u}_{sin}(y, s) = iG_1(y, s) + (1 - e^{-s}) H_1(y, s) \tag{11}$$

$$\bar{u}_{cos}(y, s) = G_1(y, s) + (1 - e^{-s}) H_1(y, s) \tag{12}$$

Solutions for Plate with Ramped Temperature:

$$\bar{\theta} = F_7(y,s) \quad (13)$$

$$\bar{C} = F_{11}(y,s)(1-e^{-s}) \quad (14)$$

$$\bar{u}_{sin}(y,s) = iG_1(y,s) + G_5(y,s) + G_6(y,s)(1-e^{-s}) - G_7(y,s) - G_4(y,s)(1-e^{-s}) \quad (15)$$

$$\bar{u}_{cos}(y,s) = G_1(y,s) + G_5(y,s) + G_6(y,s)(1-e^{-s}) - G_7(y,s) - G_4(y,s)(1-e^{-s}) \quad (16)$$

$$H_1(y,s) = G_2(y,s) - G_3(y,s) - G_4(y,s) \quad (17)$$

$$G_1(y,s) = \frac{1}{2}F_1(y,s) - \frac{1}{2}F_2(y,s) \quad (18)$$

$$G_2(y,s) = d_{17}F_3(y,s) + d_{18}F_4(y,s) + d_{12}F_5(y,s) + d_{15}F_6(y,s) \quad (19)$$

$$G_3(y,s) = d_{13}F_7(y,s) + d_{11}F_8(y,s) + d_{12}F_9(y,s) \quad (20)$$

$$G_4(y,s) = d_{16}F_{10}(y,s) + d_{14}F_{11}(y,s) + d_{15}F_{12}(y,s) \quad (21)$$

$$G_5(y,s) = d_{11}F_3(y,s) - d_{11}F_3(y,s) \quad (22)$$

$$G_6(y,s) = d_{16}F_3(y,s) + d_{14}F_4(y,s) + d_{15}F_6(y,s) \quad (23)$$

$$G_7(y,s) = d_{11}F_7(y,s) - d_{11}F_9(y,s) \quad (24)$$

$$F_1(y,s) = \frac{e^{-y\sqrt{\frac{s+d_2}{d_1}}}}{s+iw} \quad (25)$$

$$F_2(y,s) = \frac{e^{-y\sqrt{\frac{s+d_2}{d_1}}}}{s-iw} \quad (26)$$

$$F_3(y,s) = \frac{e^{-y\sqrt{\frac{s+d_2}{d_1}}}}{s} \quad (27)$$

$$F_4(y,s) = \frac{e^{-y\sqrt{\frac{s+d_2}{d_1}}}}{s^2} \quad (28)$$

$$F_5(y,s) = \frac{e^{-y\sqrt{\frac{s+d_2}{d_1}}}}{s-d_6} \quad (29)$$

$$F_6(y,s) = \frac{e^{-y\sqrt{\frac{s+d_2}{d_1}}}}{s-d_9} \quad (30)$$

$$F_7(y,s) = \frac{e^{-y\sqrt{s/a_4}}}{s} \quad (31)$$

$$F_8(y,s) = \frac{e^{-y\sqrt{s/a_4}}}{s^2} \quad (32)$$

$$F_9(y,s) = \frac{e^{-y\sqrt{s/a_4}}}{s-d_6} \quad (33)$$

$$F_{10}(y,s) = \frac{1}{s}e^{-y\sqrt{s_c\,s}} \quad (34)$$

$$F_{11}(y,s) = \frac{1}{s^2}e^{-y\sqrt{s_c\,s}} \quad (35)$$

$$F_{12}(y,s) = \frac{1}{s-d_9}e^{-y\sqrt{s_c\,s}} \quad (36)$$

Inverse Laplace transform of equation (9-36) we get

$$\theta(y,t) = f_8(y,t) - f_8(y,t-1)H(t-1) \quad (37)$$

$$C(y,t) = f_{11}(y,t) - f_{11}(y,t-1)H(t-1) \quad (38)$$

$$u_{sin}(y,t) = ig_1(y,t) + h_1(y,t-1)H(t-1) \quad (39)$$

$$u_{cos}(y,t) = g_1(y,t) + h_1(y,t-1)H(t-1) \quad (40)$$

Solutions for Plate with Constant Temperature:

In order to understand effects of ramped temperature of the plate on the fluid flow, we must compare our results with constant temperature. In this case, the initial and boundary conditions are the same excluding Eq. (8) that becomes

$$\theta = 1 \; at \; y = 0, t \geq 0$$

We find the isothermal temperature and velocity profile u (y , t) using Laplace transform technique.

$$\theta(y,t) = f_7(y,t) \tag{41}$$

Similarly, Velocity for plate with constant temperature using the Laplace transforms technique

$$u_{sin}(y,t) = ig_1(y,t) + g_5(y,t) + g_6(y,t) - g_6(y,t-1)H(t-1) - g_7(y,t) - g_4(y,t) + g_4(y,t-1)H(t-1) \tag{42}$$

$$u_{cos}(y,t) = g_1(y,t) + g_5(y,t) + g_6(y,t) - g_6(y,t-1)H(t-1) - g_7(y,t) - g_4(y,t) + g_4(y,t-1)H(t-1) \tag{43}$$

Where

$$h_1(y,t) = g_2(y,t) - g_3(y,t) - g_4(y,t) \tag{44}$$

$$g_1(y,s) = \frac{1}{2}f_1(y,t) - \frac{1}{2}f_2(y,t) \tag{45}$$

$$g_2(y,t) = d_{17}f_3(y,t) + d_{18}f_4(y,t) + d_{12}f_5(y,t) + d_{15}f_6(y,t) \tag{46}$$

$$g_3(y,t) = d_{13}f_7(y,t) + d_{11}f_8(y,t) + d_{12}f_9(y,t) \tag{47}$$

$$g_4(y,t) = d_{16}f_{10}(y,t) + d_{14}f_{11}(y,t) + d_{15}f_{12}(y,t) \tag{48}$$

$$g_5(y,t) = d_{11}f_3(y,t) - d_{11}f_3(y,t) \tag{49}$$

$$g_6(y,t) = d_{16}f_3(y,t) + d_{14}f_4(y,t) + d_{15}f_6(y,t) \tag{50}$$

$$g_7(y,t) = d_{11}f_7(y,t) - d_{11}f_9(y,t) \tag{51}$$

$$f_1(y,t) = \frac{e^{-iwt}}{2}\left[e^{-y\sqrt{\frac{1}{d_1}(d_2-iw)}}\, erfc\left(\frac{y}{2\sqrt{d_1 t}} - \sqrt{(d_2-iw)t}\right) + e^{y\sqrt{\frac{1}{d_1}(d_2-iw)}}\, erfc\left(\frac{y}{2\sqrt{d_1 t}} + \sqrt{(d_2-iw)t}\right)\right] \tag{52}$$

$$f_2(y,t) = \frac{e^{iwt}}{2}\left[e^{-y\sqrt{\frac{1}{d_1}(d_2+iw)}}\, erfc\left(\frac{y}{2\sqrt{d_1 t}} - \sqrt{(d_2+iw)t}\right) + e^{y\sqrt{\frac{1}{d_1}(d_2+iw)}}\, erfc\left(\frac{y}{2\sqrt{d_1 t}} + \sqrt{(d_2+iw)t}\right)\right] \tag{53}$$

$$f_3(y,t) = \frac{1}{2}\left[e^{-y\sqrt{\frac{d_2}{d_1}}}\, erfc\left(\frac{y}{2\sqrt{d_1 t}} - \sqrt{d_2 t}\right) + e^{y\sqrt{\frac{d_2}{d_1}}}\, erfc\left(\frac{y}{2\sqrt{d_1 t}} + \sqrt{d_2 t}\right)\right] \tag{54}$$

$$f_4(y,t) = \frac{1}{2}\left[\left(t - \frac{y}{2\sqrt{d_2 d_1}}\right)e^{-y\sqrt{\frac{d_2}{d_1}}}\, erfc\left(\frac{y}{2\sqrt{d_1 t}} - \sqrt{d_2 t}\right) + \left(t + \frac{y}{2\sqrt{d_2 d_1}}\right)e^{y\sqrt{\frac{d_2}{d_1}}}\, erfc\left(\frac{y}{2\sqrt{d_1 t}} + \sqrt{d_2 t}\right)\right] \tag{55}$$

$$f_5(y,t) = \frac{e^{d_6 t}}{2}\left[e^{-y\sqrt{\frac{1}{d_1}(d_6+d_2)}}\, erfc\left(\frac{y}{2\sqrt{d_1 t}} - \sqrt{(d_6+d_2)t}\right) + e^{-y\sqrt{\frac{1}{d_1}(d_6+d_2)}}\, erfc\left(\frac{y}{2\sqrt{d_1 t}} + \sqrt{(d_6+d_2)t}\right)\right] \tag{56}$$

$$f_6(y,t) = \frac{e^{d_9 t}}{2}\left[e^{-y\sqrt{\frac{1}{d_1}(d_9+d_2)}}\, erfc\left(\frac{y}{2\sqrt{d_1 t}} - \sqrt{(d_9+d_2)t}\right) + e^{-y\sqrt{\frac{1}{d_1}(d_9+d_2)}}\, erfc\left(\frac{y}{2\sqrt{d_1 t}} + \sqrt{(d_9+d_2)t}\right)\right] \tag{57}$$

$$f_7(y,t) = erfc\left(\frac{y}{2\sqrt{a_4 t}}\right) \tag{58}$$

$$f_8(y,t) = \left(\frac{y^2}{2a_4} + t\right) erfc\left(\frac{y}{2\sqrt{a_4 t}}\right) - \frac{y\sqrt{t}}{2\sqrt{a_4 \pi}}\, e^{-\frac{y^2}{4ta_4}} \tag{59}$$

$$f_9(y,t) = \frac{e^{d_6 t}}{2}\left[e^{-y\sqrt{\frac{d_6}{a_4}}}\, erfc\left(\frac{y}{2\sqrt{a_4 t}} - \sqrt{d_6 t}\right) + e^{y\sqrt{\frac{d_6}{a_4}}}\, erfc\left(\frac{y}{2\sqrt{a_4 t}} + \sqrt{d_6 t}\right)\right] \tag{60}$$

$$f_{10}(y,t) = erfc\left(\frac{y\sqrt{Sc}}{2\sqrt{t}}\right) \quad (61)$$

$$f_{11}(y,t) = \left(\frac{y^2 Sc}{2} + t\right) erfc\left(\frac{y\sqrt{Sc}}{2\sqrt{t}}\right) - \frac{y\sqrt{Sc\,t}}{2\sqrt{\pi}} e^{-\frac{y^2 Sc}{4t}} \quad (62)$$

$$f_{12}(y,t) = \frac{e^{d_9 t}}{2}\left[e^{-y\sqrt{Sc\,d_9}}\, erfc\left(\frac{y\sqrt{Sc}}{2\sqrt{t}} - \sqrt{d_9 t}\right) + e^{y\sqrt{Sc\,d_9}}\, erfc\left(\frac{y\sqrt{Sc}}{2\sqrt{t}} + \sqrt{d_9 t}\right)\right] \quad (63)$$

Where $u_{sin}(y,t)\ and\ u_{cos}(y,t)$ are the velocity profiles for sine and cosine oscillations for the ramped and isothermal temperatures respectively.

Nusselt Number:

The Nusselt number Nu can be written as

$$N_u = -\left(\frac{\partial\theta}{\partial y}\right)_{y=0} \quad (64)$$

Using the equation (37), we obtained the Nusselt number for Ramped wall temperature is

$$N_u = -[I_8(t) - I_8(t-1)H(t-1)] \quad (65)$$

Using the equation (41), we obtained the Nusselt number for Isothermal temperature is

$$N_u = -[I_7(t)] \quad (66)$$

Sherwood Number:

Sherwood Number is defined and denoted by the formula

$$s_h = -\left(\frac{\partial C}{\partial y}\right)_{y=0} \quad (67)$$

Using the equation (38), we obtained the Sherwood Number is

$$s_h = -[I_{11}(t) - I_{11}(t-1)H(t-1)] \quad (68)$$

Skin Friction:

Expressions of skin-friction for both cases are calculated from Equations. (39-40) and (42-43) using the relations

$$\tau^*(y,t) = -\tau \quad (69)$$

Where $\tau = \left.\frac{\partial u}{\partial y}\right|_{y=0}$ (70)

For ramped wall temperature

$$\tau_{sin}(y,t) = iI_{13}(t) + I_{20}(t) - I_{20}(t-1)H(t-1) \quad (71)$$

$$\tau_{cos}(y,t) = I_{13}(t) + I_{20}(t) - I_{20}(t-1)H(t-1) \quad (72)$$

For isothermal temperature

$$\tau_{sin}(y,t) = iI_{13}(t) + I_{17}(t) + I_{18}(t) - I_{18}(t-1)H(t-1) - I_{19}(t) - I_{16}(t) + I_{16}(t-1)H(t-1) \quad (73)$$

$$\tau_{cos}(y,t) = I_{13}(t) + I_{17}(t) + I_{18}(t) - I_{18}(t-1)H(t-1) - I_{19}(t) - I_{16}(t) + I_{16}(t-1)H(t-1) \quad (74)$$

Where

$$I_{13}(y,s) = \frac{1}{2}I_1(t) - \frac{1}{2}I_2(t) \quad (75)$$

$$I_{14}(t) = d_{17}I_3(t) + d_{18}I_4(t) + d_{12}I_5(t) + d_{15}I_6(t) \quad (76)$$

$$I_{15}(t) = d_{13}I_7(t) + d_{11}I_8(t) + d_{12}I_9(t) \quad (77)$$

$$I_{16}(t) = d_{16}I_{10}(t) + d_{14}I_{11}(t) + d_{15}I_{12}(t) \quad (78)$$

$$I_{17}(t) = d_{11}I_3(t) - d_{11}I_3(t) \quad (79)$$

$$I_{18}(t) = d_{16}I_3(t) + d_{14}I_4(t) + d_{15}I_6(t) \quad (80)$$

$$I_{19}(t) = d_{11}I_7(t) - d_{11}I_9(t) \quad (81)$$

$$I_{20}(t) = I_{14}(t) - I_{15}(t) - I_{16}(t) \quad (82)$$

$$I_1(t) = e^{-iwt}\sqrt{\frac{d_2 - iw}{d_1}}\,\mathrm{erf}\left(\sqrt{(d_2 - iw)t}\right) + \frac{e^{-d_2 t}}{\sqrt{\pi d_1 t}} \quad (83)$$

$$I_2(t) = e^{iwt}\sqrt{\frac{d_2 + iw}{d_1}}\,\mathrm{erf}\left(\sqrt{(d_2 + iw)t}\right) + \frac{e^{-d_2 t}}{\sqrt{\pi d_1 t}} \quad (84)$$

$$I_3(t) = -\sqrt{\frac{d_2}{d_1}}\,\mathrm{erf}\left(\sqrt{d_2 t}\right) + \frac{e^{-d_2 t}}{\sqrt{\pi d_1 t}} \tag{85}$$

$$I_4(t) = -\frac{1}{\sqrt{4 d_2 d_1}}\,\mathrm{erf}\left(\sqrt{d_2 t}\right) - t\sqrt{\frac{d_2}{d_1}}\,\mathrm{erf}\left(\sqrt{d_2 t}\right) + \sqrt{\frac{t}{\pi d_1}}\,e^{-d_2 t} \tag{86}$$

$$I_5(t) = e^{d_6 t}\sqrt{\frac{d_2 + d_6}{d_1}}\,\mathrm{erf}\left(\sqrt{(d_2 + d_6)t}\right) + \frac{e^{-d_2 t}}{\sqrt{\pi d_1 t}} \tag{87}$$

$$I_6(t) = e^{d_9 t}\sqrt{\frac{d_2 + d_9}{d_1}}\,\mathrm{erf}\left(\sqrt{(d_2 + d_9)t}\right) + \frac{e^{-d_2 t}}{\sqrt{\pi d_1 t}} \tag{88}$$

$$I_7(t) = \sqrt{\frac{1}{\pi a_4 t}} \tag{89}$$

$$I_8(t) = \frac{1}{2}\sqrt{\frac{t}{\pi a_4}} \tag{90}$$

$$I_9(t) = -e^{d_6 t}\sqrt{\frac{d_6}{a_4}}\,\mathrm{erf}\left(\sqrt{d_6 t}\right) + \sqrt{\frac{1}{\pi a_4 t}} \tag{91}$$

$$I_{10}(t) = \sqrt{\frac{Sc}{\pi t}} \tag{92}$$

$$I_{11}(t) = \frac{1}{2}\sqrt{\frac{tSc}{\pi}} \tag{93}$$

$$I_{12}(t) = -e^{d_9 t}\sqrt{Sc\, d_9}\,\mathrm{erf}\left(\sqrt{d_9 t}\right) + \sqrt{\frac{Sc}{\pi t}} \tag{94}$$

IV. FIGURES

In this section, to get a clear insight on the physics of the problem, the obtained exact solutions are studied numerically and are elucidated with the help of graphs. Parametric study is performed for Prandtl number Pr, Grashof number Gr, mass Grashof number Gm, magnetic parameter M, Schmidt number.

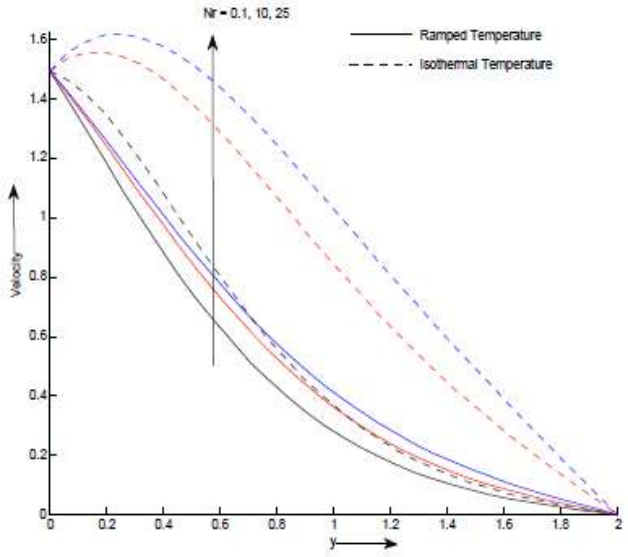

Figure 2. Velocity profile for different values of y and Nr at
$t = 0.4$ M $= 0.5$ $G_r = 10$ $\emptyset = 0.02$ $p_r = 7$

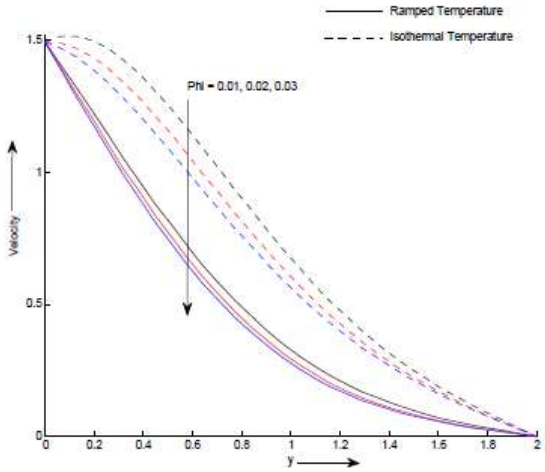

Figure 3. Velocity profile u for different values of y and $\emptyset$ at $w = \pi, Pr = 7, M = 0.5, Sc = 0.66, Gm = 5, Gr = 10, k = 1$ and $t = 0.4$

Sc, permeability of porous medium K, phase angle , volume fraction parameter and time t in Figures. 2-16. Numerical values of skin-friction Nusselt number and Sherwood number Nu are computed and presented in tables for different parameters

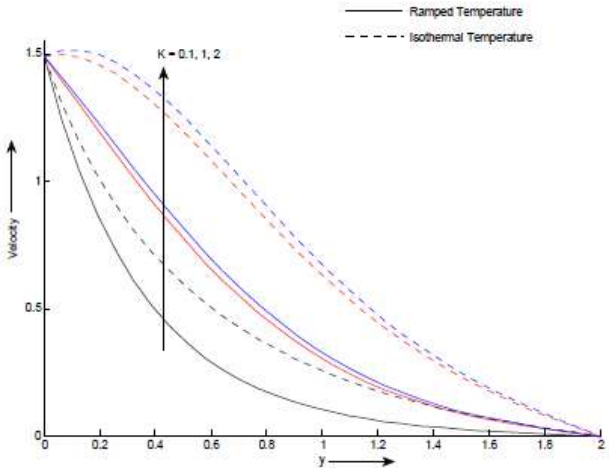

Figure 4. Velocity profile u for different values of y and k at $w = \pi, Pr = 7, M = 0.5, Sc = 0.66, Gm = 5, Gr = 10, \emptyset = 0.02$ and $t = 0.4$

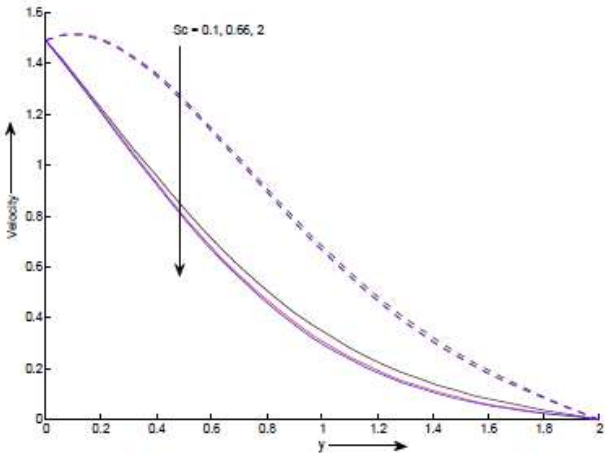

Figure 5. Velocity profile u for different values of y and Sc at $w = \pi, Pr = 7, M = 0.5, k = 1, Gm = 5, Gr = 10, \emptyset = 0.02$ and $t = 0.4$

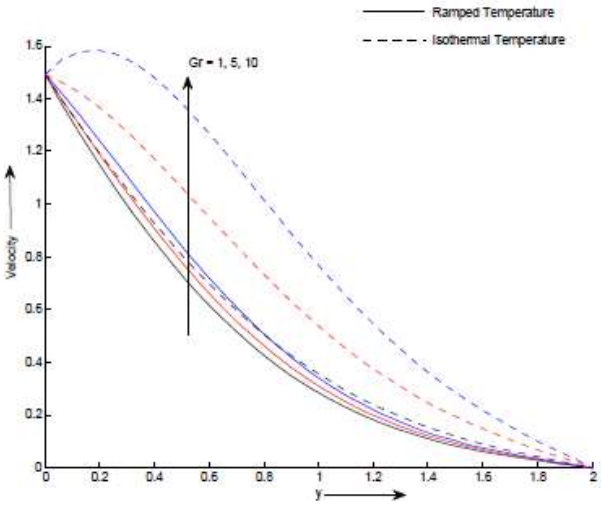

Figure 6. Velocity profile u for different values of y and Gr at $w = \pi, Pr = 7, M = 0.5, k = 1, Sc = 0.66, Gm = 5, \emptyset = 0.02$ and $t = 0.4$

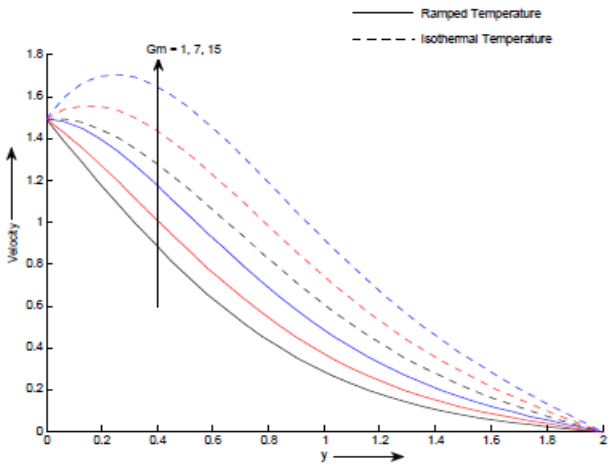

Figure 7. Velocity profile u for different values of y and Gm at $w = \pi, Pr = 7, M = 0.5, k = 1, Sc = 0.66, Gr = 10, \emptyset = 0.02$ and $t = 0.4$

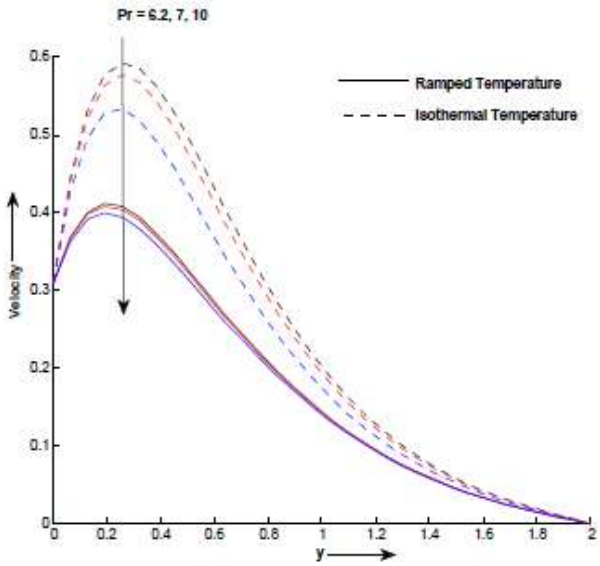

Figure 8. Velocity profile u for different values of y and Pr at $w = \pi, Gr = 10, M = 0.5, k = 1, Sc = 0.66, Gm = 5, \emptyset = 0.02$ and $t = 0.4$

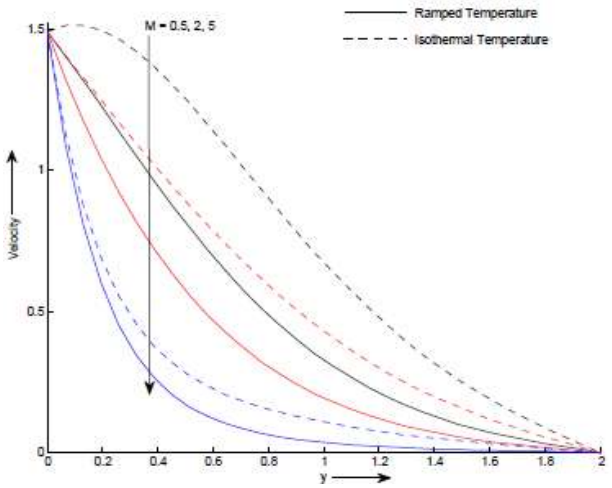

Figure 9. Velocity profile u for different values of y and M at $\mathbf{w = \pi, Gr = 10, Pr = 7, k = 1, Sc = 0.66, Gm = 5, \emptyset = 0.02}$ **and** $\mathbf{t = 0.4}$

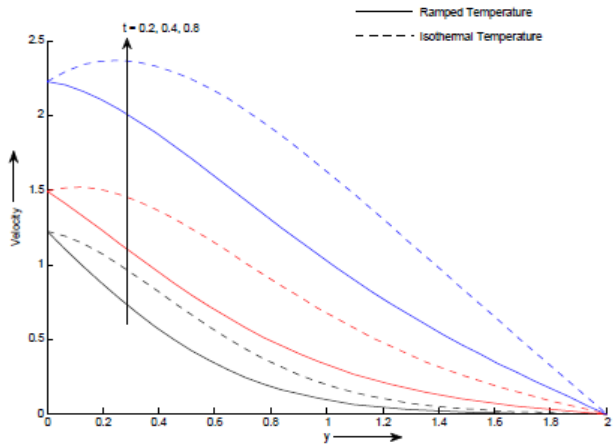

Figure 10. Velocity profile u for different values of y and t at $\mathbf{w = \pi, Gr = 10, Pr = 7, k = 1, Sc = 0.66, Gm = 5, \emptyset = 0.02}$

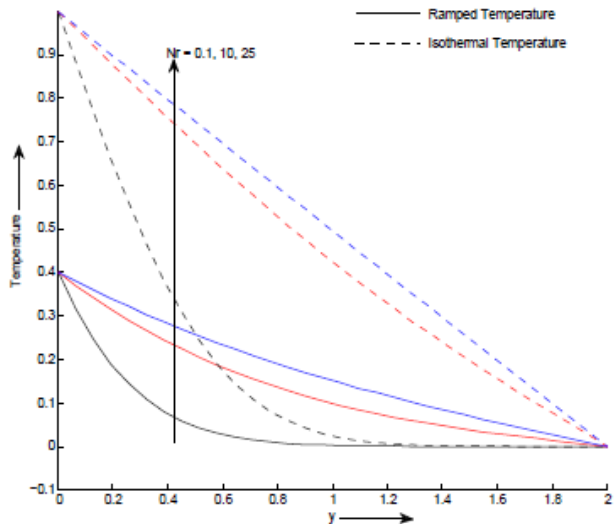

Figure 11. Temperature profile for different values of y and N_r at $M = 0.5\ t = 0.4\ \emptyset = 0.02\ G_r = 10\ p_r = 7$

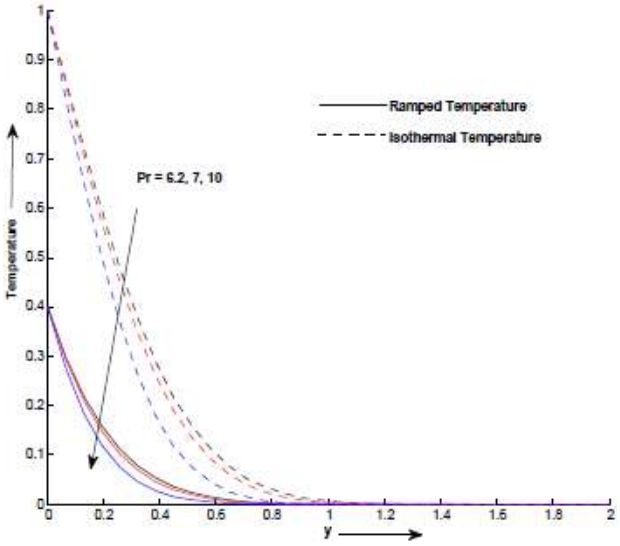

Figure 12. Temperature profile θ for different values of y and **P**r at $\emptyset = 0.02$ and $t = 0.4$

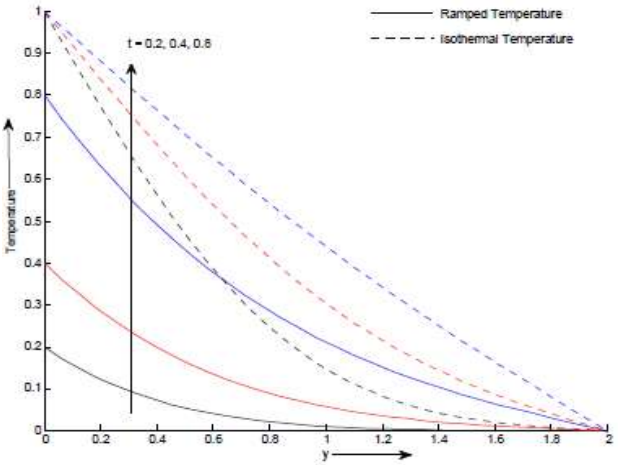

Figure 13. Temperature profile θ for different values of y and t at $\emptyset = 0.02$ and $Pr = 7$

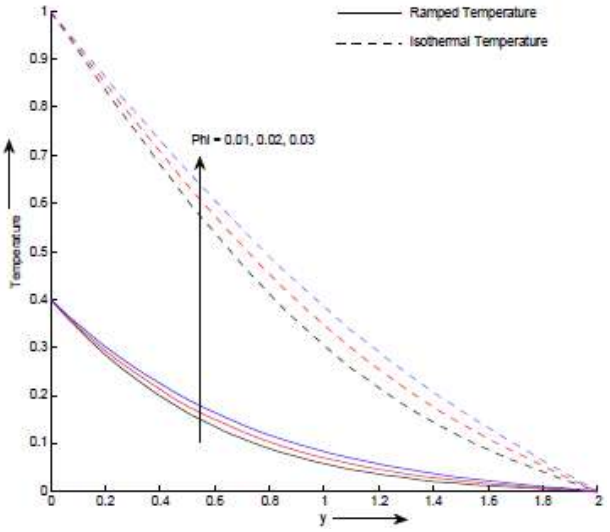

Figure 14. Temperature profile θ for different values of y and $\emptyset$ at $Pr = 7$

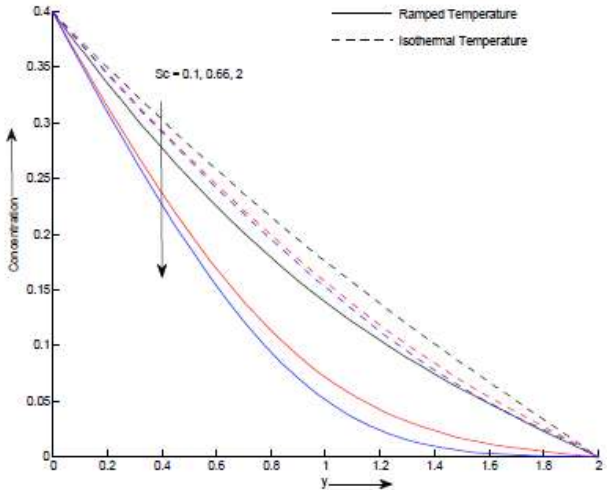

Fig 15: Concentration profile C for different values of y and Sc at $t = 0.4$

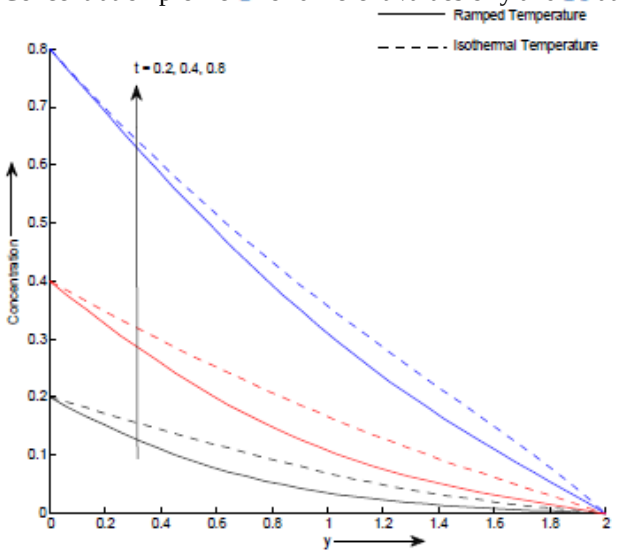

Fig 16: Concentration profile C for different values of y and t

V. TABLES

Table 1: Nusselt number variation

Ø	Pr	T	Nu for Ramped Temperature	Nu for isothermal Temperature
0.01	6.2	0.4	-0.2705	-1.6473
0.02	6.2	0.4	-0.2441	-1.5160
0.03	6.2	0.4	-0.2202	-1.3956
0.03	7.2	0.4	-0.2501	-1.5476
0.03	8.2	0.4	-0.2789	-1.6874
0.03	6.2	0.5	-0.2575	-1.2272
0.03	6.2	0.6	-0.2920	-1.1031

Table 2: Skin friction variation

Ø	Pr	M	Sc	Gr	Gm	k	t	Skin friction τ for Ramped temperature	Skin friction τ for isothermal temperature
0.01	6.2	0.5	1.5	10	5	0.6	0.4	-9.0312	-2.6142
0.03	6.2	0.5	1.5	10	5	0.6	0.4	-6.0127	-1.9989
0.02	6.2	0.5	1.5	10	5	0.6	0.4	-4.2085	-1.5229
0.02	7.2	0.5	1.5	10	5	0.6	0.4	-4.7238	-1.4707
0.02	8.2	0.5	1.5	10	5	0.6	0.4	-5.2974	-1.4288
0.02	6.2	0.6	1.5	10	5	0.6	0.4	-4.0237	-1.4535
0.02	6.2	0.7	1.5	10	5	0.6	0.4	-3.6355	-1.3833
0.02	6.2	0.5	2	10	5	0.6	0.4	-4.6707	-1.9843
0.02	6.2	0.5	2.5	10	5	0.6	0.4	-5.0823	-2.4937
0.02	6.2	0.5	1.5	11	5	0.6	0.4	-4.5765	-1.6212
0.02	6.2	0.5	1.5	12	5	0.6	0.4	-5.0456	-1.7209
0.02	6.2	0.5	1.5	10	6	0.6	0.4	-4.5363	-1.8499
0.02	6.2	0.5	1.5	10	7	0.6	0.4	-4.8542	-2.1764
0.02	6.2	0.5	1.5	10	5	0.7	0.4	-4.4688	-1.5851
0.02	6.2	0.5	1.5	10	5	0.8	0.4	-4.7343	-1.6445
0.02	6.2	0.5	1.5	10	5	0.6	0.5	-5.3401	-2.0537
0.02	6.2	0.5	1.5	10	5	0.6	0.6	-6.4700	-2.5828

Table 3. Sherwood Number variation

Sc	t	Sherwood Number Sh
1.2	0.5	-0.2107
2.3	0.5	-0.2441
2.8	0.5	-0.2749
1.2	0.6	-0.2362
1.2	0.7	-0.2599

VI. RESULTS AND DISCUSSION

Physical sketch of the problem is shown in Figure 1. Figure 2 Illustrates the velocity profile for different values of Nr. It is noticed that the fluid velocity u increase with radiation parameter Nr. Figure 3 displays the effect of volume fraction of nanoparticles on nanofluid velocity. The nanofluid velocity increases as volume fraction parameter decreases. Figure 4 shows that velocity increases with increase in K. Increase in K results in decrease in the resistance of the porous medium which increases the momentum of the flow regime, enhancing the velocity field. Figure 5 depicts the effect of Schimdt number Sc on the nanofluid velocity. The nanofluid velocity decreases for increasing values of Sc. Figure 6 and Figure 7 illustrate that increase in Grashof number Gr and mass Grashof number Gm result in accelerated velocity. Grashof number is the ratio of the buoyancy force due to variation in nanofluid density (caused by temperature differences) to the restraining force due to the viscosity of the nanofluid. Positive Gr accelerates the nanofluid in the boundary layer resulting increase in the velocity. Figure 8 exhibits that velocity of the nanofluid decreases with increase in Prandtl number. It is due to decrease in thermal conductivity of the nanofluid with increase in Pr. Figure 9 reveals that the nanofluid velocity decreases for increasing magnetic parameter M. Physically, it is due to the transverse magnetic field resulting in resistive Lorentz force and upon increasing the values of M, this drag force increases leading to the deceleration of the flow. Figure 10 exhibits that nanofluid velocity increases with increasing volume of fraction of nanoparticles. Figure 11 reveals that temperature decreases with increase in radiation parameter as release of heat energy from the region is also increased. Decrease in the Rosseland radiation absorptivity is also observed with Nr resulting divergence of the radiative heat flux. This increases in rate of radiative heat transfer to the fluid and hence the fluid temperature increases. Figure 12 represents that the nanofluid temperature decreases as Pr increases. It is due to decreased thermal conductivity of the nanofluid with increasing Prandtl number Pr. Figure 13 reveals that nanofluid temperature increases with increase in time t. Figure 14 depicts that volume

fraction of nanoparticles has positive impact on temperature profile. It is evident from Figure 15 that, *C* increases on increasing *Sr* throughout the boundary layer region. Figure 16 illustrates the effect of time on the species concentration. It is perceived from Figure 16, *C* increases on increasing *t*. This implies that, species concentration is getting enhanced.

The numerical values of Nusselt number Nu, skin friction s and Sherwood number Sh are exhibited in tabular form in Table 1, Tables 2 and Table 3 respectively. It is clear from Table 1 that, Nu decreases for ramped temperature and increases for isothermal case as time passes. Table 2 depicts that, skin friction reduces with passage of time for both ramped and isothermal temperature plate. Table also illustrates that the skin friction can be decreased by increasing Gr or Gm or Sc or K. It is evident from Table 3 that Sherwood number increases with decrease in value of t or Sc for both plate temperature cases.

VII. CONCLUSION

The most important concluding remarks can be summarized as follows:

- Nanofluid velocity is getting accelerated with the progress of Grashof number Gr, mass Grashof number Gm and time t while decreases with increase in Pr, M and Sc.
- The velocity of the nanofluid increases with increase in Nr for different frequencies of oscillation ω of the plate.
- Nanofluid velocity is more for isothermal temperature compared to ramped plate.
- Nanofluid temperature tends to increase with rise in values of Prandtl number Pr and time t.
- Nanofluid temperature decreases with increase in the radiation parameter Nr.
- Concentration decreases with increase in Schimdt number Sc while increase with progress of time.
- Nusselt number Nu decreases on increasing t for ramped temperature and otherwise for isothermal case.
- Sherwood number decreases with increase in t or Sc for both ramped temperature and isothermal plate.
- Nanofluid velocity decreases with increase in volume fraction parameter $\emptyset$.
- Skin friction and Nusselt number increase with increase in Nr.
- Skin friction and Nu increases with increase in volume fraction parameter $\emptyset$.

REFERENCES

[1] M. Narahari, O. A. Beg and S. K. Ghosh, Mathematical modeling of mass transfer and free convection current effects on unsteady viscous flow with ramped wall temperature, World J. Mech., 1(2011) 176–184.

[2] M. Narahari, Transient free convection flow between long vertical parallel plates with ramped wall temperature at one boundary in the presence of thermal radiation and constant mass diffusion, Meccanica, 47, (2012) 1961–1976.

[3] M. Narahari and S. A. Sulaiman, Thermal radiation effects on unsteady MHD natural convection flow past an infinite inclined plate with ramped temperature, Adv. Sci. Lett., 19(2012), 296-300.

[4] S. Nadeem, R. Haq, C. Lee, MHD flow of a Casson fluid over an exponentially shrinking sheet, Scientia Iranica, 19(6), (2012)1550-1553.

[5] G.S. Seth, R. Nandkeolyar, Md. S. Ansari, Effects of Thermal Radiation and Rotation on Unsteady Hydromagnetic Free Convection Flow Past an Impulsively Moving Vertical Plate with Ramped Temperature in a Porous Medium, J. Appl. Fluid Mech, 6 (1) (2013) 27-38.

[6] G. S. Seth, G. K. Mahato , S. Sarkar, Effects of Hall Current and Rotation on MHD Natural Convection Flow Past an Impulsively Moving Vertical Plate with Ramped Temperature in the Presence of Thermal Diffusion with Heat Absorption, Int. J. Energy & Tech, 5 (16) (2013) 1- 12.

[7] G. S. Seth, S. Sarkar, G. K. Mahato, Effects of Hall Current on Hydromagnetic Free Convection Flow with Heat And Mass Transfer of a Heat Absorbing Fluid Past an Impulsively Moving Vertical Plate with Ramped Temperature, Int. J. Heat Tech 31 (1) (2013) 85-96.

[8] G. S. Seth, S. Sarkar, S. M. Hussain , Effects of Hall current Radiation and Rotation on Natural Convection Heat and Mass Transfer Flow Past a Moving Vertical Plate, Ain Shams Engineering Journal 5 (2) (2014) 489-503.

[9] G. S. Seth, S. M. Hussain, S. Sarkar, Effects of Hall current and Rotation on Unsteady MHD Natural Convection Flow with Heat and Mass Transfer Past an Impulsively Moving Vertical Plate in the Presence of Radiation and Chemical Reaction, Bulg, Chem. Comm, 46 (4) (2014) 704- 718.

[10] G. S. Seth, B. Kumbhakar, S. Sarkar, Unsteady Hydromagnetic Natural Convection Flow With Heat and Mass Transfer of a Thermally Radiating and Chemically Reactive Fluid Past a Vertical Plate with Newtonian Heating and Time Dependent Free-Stream, Int. J. Heat Tech, 32 (1-2) (2014) 87-94.

[11] G. S. Seth, R. Sharma, S. Sarkar, Hydromagnetic Natural Convection Heat and Mass Transfer Flow with Hall Current of a Heat Absorbing and Radiating Fluid Past an Accelerated Moving Vertical Plate with Ramped Temperature in a Rotating Medium, J. Appl. Fluid Mech 8 (1) (2015) 7-20.

[12] G. S. Seth, S. Sarkar, S. M. Hussain, G. K. Mahato, Effects of Hall Current and Rotation on Hydromagnetic Natural Convection Flow with Heat and Mass Transfer of a Heat Absorbing Fluid Past an Impulsively Moving Vertical Plate with Ramped Temperature, J. Appl. Fluid Mech 8 (1) (2015),159- 171.

[13] G. S. Seth, S. Sarkar, MHD Natural Convection Heat and Mass Transfer Flow Past a Time Dependent Moving Vertical Plate with Ramped Temperature in a Rotating Medium with Hall Effects, Radiation and Chemical Reaction, J. Mech 31 (2015) 91 – 104

[14] M. Naraharii, T. Sowmya and R. Pendyala, Ramp temperature and Dufour effects on transient MHD natural convection flow past an infinite vertical plate in a porous medium, Eur. Phys. J. Plus. 130(2015) 251.

[15] G. S. Seth, B. Kumbhakar, R. Sharma, Unsteady MHD free convection flow with Hall effect of a radiating and heat absorbing fluid past a moving vertical plate with variable ramped temperature, Journal of the Egyptian Mathematical Society 24 (3) (2016), 471–

478
[16] R. Mehmood, S. Nadeem, S. Masood, Effects of transverse magnetic field on a rotating micropolar fluid between parallel plates with heat transfer, Journal of Magnetism and Magnetic Materials, 401(1),(2016)1006-1014
[17] S. Nadeem, N. Muhammad, Impact of stratification and Cattaneo-Christov heat flux in the flow saturated with porous medium, Journal of Molecular Liquids, 224(A), (2016)423-430
[18] S. R. Sheri, A. K. Suram, P. Modulgua, Heat and mass transfer effects on mhd natural convection flow past an infinite inclined plate with ramped temperature, Journal Of The Korean Society For Industrial And Applied Mathematics 20 (4), (2016)355-374
[19] S. R. Sheri, R. S. Raju, Transient MHD free convective flow past an infinite vertical plate embedded in a porous medium with viscous dissipation, Meccanica 51 (5), (2016)1057-1068
[20] H. Kataria, H. Patel, Heat and Mass Transfer in MHD Second Grade Fluid Flow with Ramped Wall Temperature through Porous Medium, Mathematics Today, 32 (2016) 67-83.
[21] H. Kataria, H. Patel, Radiation and chemical reaction effects on MHD Casson fluid flow past an oscillating vertical plate embedded in porous medium, Alexandria Engineering Journal, 55 (2016) 583–595.
[22] H. Kataria, H. Patel, soret and heat generation effects on MHD Casson fluid flow past an oscillating vertical plate embedded through porous medium, Alexandria Engineering Journal, 55 (2016) 2125–2137.
[23] H. Kataria, H. Patel, Effect of thermo-diffusion and parabolic motion on MHD Second grade fluid flow with ramped wall temperature and ramped surface concentration, Alexandria Engineering Journal, 10.1016/j.aej.2016.11.014.
[24] H. Kataria, H. Patel, R. Singh. Effect of magnetic field on unsteady natural convective flow of a micropolar fluid between two vertical walls. Ain Shams Engineering Journal, 8 (2017) 87–102.
[25] T. Hayat, M. Waqas, M. I. Khan, A. Alsaedi, S. A. Shehzad, Magnetohydrodynamic flow of burgers fluid with heat source and power law heat flux, Chinese Journal of Physics 55 (2), (2017)318-330
[26] M. Sheikholeslami, D.D. Ganji, Heat transfer of Cu-water nanofluid flow between parallel plates, Powder Technology, 235, (2013) 873-879
[27] M. Sheikholeslami, M. Hatami, D.D. Ganji, Analytical investigation of MHD nanofluid flow in a semi-porous channel, Powder Technol. 246 (2013) 327–336.
[28] M. Sheikholeslami, M. Hatami, D.D. Ganji, Micropolar fluid flow and heat transfer in a permeable channel using analytical method, J. Mol. Liq. 194 (2014) 30–36.
[29] M. Sheikholeslami, S. Abelman, D. D. Ganji, Numerical simulation of MHD nanofluid flow and heat transfer considering viscous dissipation, International Journal of Heat and Mass Transfer 79 (2014) 212–222
[30] H. R. Kataria, A. Mittal. Mathematical model for velocity and temperature of gravity-driven convective optically thick nanofluid flow past an oscillating vertical plate in presence of magnetic field and radiation. Journal of Nigerian Mathematical Society, 34 (2015) 303–317.
[31] S. R. Sheri, T. Thumma, Double Diffusive Magnetohydrodynamic Free Convective Flow of Nanofluids Past an Inclined Porous Plate Employing Tiwari and Das Model: FEM, Journal of Nanofluids 5 (6), (2016)802-816
[32] S. R. Sheri, T. Thumma, Heat and Mass Transfer Effects on Natural Convection Flow in the Presence of Volume Fraction for Copper-Water Nanofluid, Journal of Nanofluids 5 (2), (2016)220-230
[33] M. Sheikholeslami, H. R. Kataria, A. S. Mittal, Radiation effects on heat transfer of three dimensional nanofluid flow considering thermal interfacial resistance and micro mixing in suspensions, Chin. J. Phys. 2017, doi.org/10.1016/j.cjph.2017.09.010.
[34] H. R. Kataria, A. S. Mittal, Velocity, mass and temperature analysis of gravity-driven convection nanofluid flow past an oscillating vertical plate in presence of magnetic field in a porous medium, Applied Thermal Engineering, 110 (2017) 864-874.
[35] R. Mehmood, S. Nadeem, S. Saleem, N. S. Akbar, Flow and heat transfer analysis of Jeffery nano fluid impinging obliquely over a stretched plate, Journal of the Taiwan Institute of Chemical Engineers, 74, (2017) 49-58
[36] I. Shahzadi, S. Nadeem, Inclined magnetic field analysis for metallic nanoparticles submerged in blood with convective boundary condition, Journal of Molecular Liquids, 230, (2017)61-73
[37] R. Tabassum, R. Mehmood, S. Nadeem, Impact of viscosity variation and micro rotation on oblique transport of Cu-water fluid, Journal of Colloid and Interface Science, 501, (2017)304-310
[38] A. Rehman, R. Mehmood, S. Nadeem, Entropy analysis of radioactive rotating nanofluid with thermal slip, Applied Thermal Engineering, 112, (2017)832-840
[39] M. Sheikholeslami, S. A. Shehzad, Thermal radiation of ferrofluid in existence of Lorentz forces considering variable viscosity,International Journal of Heat and Mass Transfer 109, (2017)82-92
[40] A. Rauf, S. A. Shehzad, T. Hayat, M. A. Meraj, A. Alsaedi, MHD stagnation point flow of micro nanofluid towards a shrinking sheet with convective and zero mass flux conditions, Bulletin of the Polish Academy of Sciences Technical Sciences 65 (2), (2017)155-162
[41] T. Hayat, S. Qayyum, S.A. Shehzad, A Alsaedi, Magnetohydrodynamic three-dimensional nonlinear convection flow of Oldroyd-B nanoliquid with heat generation/absorption, Journal of Molecular Liquids 230, (2017)641-651.
[42] T. Hayat, T. Muhammad, S. A. Shehzad, A Alsaedi, Three dimensional rotating flow of Maxwell nanofluid, Journal of Molecular Liquids 229, (2017)495-500
[43] T. Hayat, T. Muhammad, S. A. Shehzad, A. Alsaedi, On magnetohydrodynamic flow of nanofluid due to a rotating disk with slip effect: A numerical study, Computer Methods in Applied Mechanics and Engineering 315, (2017)467-477
[44] T. Hayat, T. Muhammad, S. A. Shehzad, A. Alsaedi, An analytical solution for magnetohydrodynamic Oldroyd-B nanofluid flow induced by a stretching sheet with heat generation/absorption, International Journal of Thermal Sciences 111, (2017)274-288
[45] H.F. Oztop, E. Abu-Nada, Numerical study of natural convection in partially heated rectangular enclosures filled with nanofluids, Int. J. Heat Fluid Flow 29 (2008) 1326–1336.
[46] J. Koo, C. Kleinstreuer, Laminar nanofluid flow in microheat-sinks, Int. J. Heat Mass Transfer 48 (2005) 2652–2661.
[47] J. Koo, C. Kleinstreuer, Viscous dissipation effects in micro tubes and micro channels, Int. J. Heat Mass Transfer 47 (2004) 3159–3169.
[48] S. Rosseland, Astrophysik und atom-theoretischeGrundlagen, Springer-Verlag, Berlin, 1931.

Appendix:

$$d_1 = a_1 \qquad d_2 = a_3 M^2 + \frac{a_1}{k} \qquad d_3 = Gr\ a_2$$

$$d_4 = Gm\ a_5 \qquad d_5 = \frac{d_1}{a_4} - 1 \qquad d_6 = \frac{d_2}{d_5}$$

$$d_7 = \frac{d_3}{d_5} \qquad d_8 = d_1 Sc - 1 \qquad d_9 = \frac{d_2}{d_8}$$

$$d_{10} = \frac{d_4}{d_8} \qquad d_{11} = -\frac{d_7}{d_6} \qquad d_{12} = \frac{d_7}{{d_6}^2}$$

$$d_{13} = \frac{d_7}{(1-d_6)} - d_{11} - \frac{d_{12}}{(1-d_6)} \qquad d_{14} = -\frac{d_{10}}{d_9} \qquad d_{15} = \frac{d_{10}}{{d_9}^2}$$

$$d_{16} = \frac{d_{10}}{(1-d_9)} - d_{14} - \frac{d_{15}}{(1-d_9)} \qquad d_{17} = d_{16} + d_{13} \qquad d_{18} = d_{11} + d_{14}$$

$$I_1 = \left.\frac{df_1}{dy}\right|_{y=0} \qquad I_2 = \left.\frac{df_2}{dy}\right|_{y=0} \qquad I_3 = \left.\frac{df_3}{dy}\right|_{y=0}$$

$$I_4 = \left.\frac{df_4}{dy}\right|_{y=0} \qquad I_5 = \left.\frac{df_5}{dy}\right|_{y=0} \qquad I_6 = \left.\frac{df_6}{dy}\right|_{y=0}$$

$$I_7 = \left.\frac{df_7}{dy}\right|_{y=0} \qquad I_8 = \left.\frac{df_8}{dy}\right|_{y=0} \qquad I_9 = \left.\frac{df_9}{dy}\right|_{y=0}$$

$$I_{10} = \left.\frac{df_{10}}{dy}\right|_{y=0} \qquad I_{11} = \left.\frac{df_1}{dy}\right|_{y=0} \qquad I_{12} = \left.\frac{df_2}{dy}\right|_{y=0}$$

$$I_{13} = \left.\frac{dg_1}{dy}\right|_{y=0} \qquad I_{14} = \left.\frac{dg_2}{dy}\right|_{y=0} \qquad I_{15} = \left.\frac{dg_3}{dy}\right|_{y=0}$$

$$I_{16} = \left.\frac{dg_4}{dy}\right|_{y=0} \qquad I_{17} = \left.\frac{dg_5}{dy}\right|_{y=0} \qquad h_{18} = \left.\frac{dg_6}{dy}\right|_{y=0}$$

$$I_{19} = \left.\frac{dg_7}{dy}\right|_{y=0} \qquad I_{20} = \left.\frac{dh_1}{dy}\right|_{y=0}$$

International Journal of Computational Engineering Research (IJCER) is UGC approved Journal with Sl. No. 4627, Journal no. 47631.

Dr. Hari R. Kataria Effect of radiation on MHD nanofluid flow considering effective thermal conductivity and viscosity due to Brownian motion." IInternational Journal of Computational Engineering Research (IJCER), vol. 7, no. 10, 2017, pp. 01-18.